The Predictability of Stratospheric Warming Events: More from the Troposphere or the Stratosphere?

LANTAO SUN

Department of Earth and Atmospheric Sciences, Cornell University, Ithaca, New York

WALTER A. ROBINSON

Department of Marine, Earth, and Atmospheric Sciences, North Carolina State University, Raleigh, North Carolina

GANG CHEN

Department of Earth and Atmospheric Sciences, Cornell University, Ithaca, New York

ABSTRACT

The roles of the stratosphere and the troposphere in determining the predictability of stratospheric final warming and sudden warming events are evaluated in an idealized atmospheric model. For each stratospheric warming event simulated in the model, a number of forecast experiments are performed from 10 or 20 days prior to the warming onset with perturbations in the troposphere and in the stratosphere separately. It is found that the stratosphere affects predictions of warming onset primarily by providing the initial state of the zonal winds, while the tropospheric initial conditions have a large impact through the generation and propagation of planetary waves. These results correspond to the roles played by the initial zonal flow and the evolution of eddy forcings in a zonally symmetric model. The initial stratospheric zonal flow has some influence on stratospheric wave driving, but in most cases this does not significantly affect the timing of the warming, except when the initial condition is close to the onset date. These results highlight the role of the troposphere in determining stratospheric planetary wave driving and support the importance of tropospheric precursors to the stratospheric warming events.

1. Introduction

The stratosphere has received increasing attention since it was recognized that the stratosphere does not respond passively to the troposphere and that knowledge of stratospheric initial conditions can contribute to tropospheric weather prediction (e.g., Baldwin et al. 2003; Charlton et al. 2003; Kuroda 2008). Stratospheric variability in the extratropics is associated with dramatic warming events in high latitudes. In some boreal winters and in the unusual austral winter of 2002, planetary waves originating from the troposphere induce an abrupt breakup of the stratospheric polar vortex (a stratospheric sudden warming), followed by a gradual recovery. In both hemispheres the polar vortex breaks down each spring

(the stratospheric final warming) and does not build up again until the following fall. Both stratospheric sudden warmings and final warmings can dynamically organize the large-scale circulation in the stratosphere and the troposphere (Baldwin and Dunkerton 2001; Black et al. 2006, hereafter BMR06). Generally speaking, increasing model resolution of the stratosphere improves the predictability of stratospheric warming events (e.g., Marshall and Scaife 2010) and therefore has the potential to improve weather forecasts in the troposphere (Roff et al. 2011).

The predictability of stratospheric warming events also has implications for chemical processes in the stratosphere. The timing of stratospheric sudden warmings and final warmings varies from year to year. The breakdown of the polar vortex mixes ozone-rich midlatitude air with high-latitude air, and thus a late final warming is associated with a slowed seasonal recovery of ozone concentrations in the polar region (e.g., Salby and Callaghan

Corresponding author address: Lantao Sun, Department of Earth and Atmospheric Sciences, Cornell University, Ithaca, NY 14853.
E-mail: ls544@cornell.edu

2007). This may serve as a dynamical feedback mechanism to the observed stratospheric ozone depletion in the late twentieth century and its associated downward influence on the troposphere (e.g., Waugh et al. 1999).

It is recognized that anomalous upward Eliassen–Palm (E–P) fluxes from the troposphere into the stratosphere play an important role in the onset of the sudden warming (e.g., Polvani and Waugh 2003; Scott and Polvani 2004) and final warming events (e.g., BMR06; Black and McDaniel 2007b; Sun and Robinson 2009; Sun et al. 2011, hereafter SRC11). It is not, however, fully understood what causes the outburst of upward E–P flux prior to the warming. While presumably the upward flux across the tropopause is largely controlled by the amplitude of the planetary waves in the troposphere, stratospheric variability can also precondition the upward flux and alter the onset of warming events (e.g., Labitzke 1981; McIntyre 1982; Robinson 1986). Scott and Polvani (2004) showed that even if the amplitude of surface forcing is constant, the upward E–P flux at the tropopause level can be strongly influenced by variability in the stratosphere. Further, Reichler et al. (2005) found large variability in the responses of the stratosphere–troposphere system to an imposed pulse of surface planetary wave forcing, due to variability in the background wind variability in both the troposphere and the stratosphere. For the case of final warming, the increased E–P flux across the tropopause is also initiated by the seasonal weakening of the polar vortex resulting from the seasonal increase in solar heating (BMR06; Black and McDaniel 2007b; Sun and Robinson 2009; SRC11). These studies provide evidence that both the stratosphere and the troposphere are important for the onset of warming events.

There are two distinct perspectives on the predictability of stratospheric warmings, with separate foci on tropospheric precursors and the internal variability of the stratosphere. Holton and Mass (1976) showed that wave–mean flow interactions within the stratosphere lead to stratospheric vacillations, a line of research continued by Yoden (1987), Christiansen (1999, 2000), and Scott and Polvani (2006) in more sophisticated stratospheric models. On the other hand, the onset of a sudden warming is attributed to anomalous wave propagation from the troposphere, and thus the predictability of the sudden warming can be traced back to the troposphere. For example, Martius et al. (2009) reported that 25 of observed 27 sudden warming events in the Northern Hemisphere (NH) are preceded by blocking events in the troposphere, and they suggested that tropospheric blocking is a necessary but not sufficient condition for the occurrence of sudden warmings. Allen et al. (2006) showed that predictions of tropospheric blocks are important for hindcasts of the 2002 Southern

Hemisphere (SH) sudden warming. Similarly, Garfinkel et al. (2010) found that the tropospheric variability in the North Pacific and over eastern Europe contributes to the variability in planetary wavenumbers 1 and 2 and thus influences the weakening of the stratospheric polar vortex. It is of interest to compare these two views in the context of a range of sudden and final warming events in a coupled stratosphere–troposphere system.

Here we use an idealized atmospheric model to evaluate the relative roles of the troposphere and the stratosphere in determining the predictability of stratospheric warming events. A common approach is to perturb the troposphere only (e.g., Reichler et al. 2005; Gerber et al. 2009) or the stratosphere only (e.g., Kushner and Polvani 2004; Song and Robinson 2004) and then examine the instantaneous or mean response in the troposphere and stratosphere. To compare the roles of the troposphere and the stratosphere, one needs to evaluate the responses of the same set of warming events to different stratospheric and tropospheric perturbations. We run a number of forecast experiments for each stratospheric warming event simulated in an idealized model, starting from 10 or 20 days prior to the warming onset. The perturbation experiments are constructed by shifting tropospheric or stratospheric initial conditions forward or backward, in time from the initial date of the forecast. The influences of the troposphere or stratosphere in the warming onset can be quantified by the change of warming onset date with respect to the change of the initial conditions in the respective regions.

This paper comprises five sections. Following the introduction, section 2 describes the idealized model and the perturbation method for the prediction experiments. The predictability is evaluated for final warmings in section 3 and sudden warmings in section 4. The final section provides conclusions and a discussion of our results.

2. Model and perturbation method

a. Idealized atmospheric model

Our model is built on the 1990s version of the Geophysical Fluid Dynamics Laboratory (GFDL) spectral atmospheric dynamical core. The model runs at the horizontal resolution of rhomboidal 30 (R30) spherical harmonic truncations and with 30 vertical pressure-sigma levels, those used by Scinocca and Haynes (1998).

Diabatic processes are parameterized by relaxing the temperature to a zonally symmetric equilibrium temperature field. In the troposphere, the equilibrium temperature is identical to those in Held and Suarez (1994). In the stratosphere, above 100 hPa, the equilibrium temperature is obtained from a prescribed zonal wind profile using

the thermal wind relation. The radiative-equilibrium zonal winds for the summer and winter hemispheres are similar to those used by Scott and Haynes (1998).

Stratospheric final warmings are simulated by imposing a seasonal cycle in the stratospheric equilibrium temperatures:

$$T_{eq}(\phi, \sigma, t) = \gamma(t) \times T_{eq}^{winter}(\phi, \sigma)$$
$$+ [1 - \gamma(t)] \times T_{eq}^{summer}(\phi, \sigma), \quad (1)$$

where $\gamma(t) = 0.5 \times [1 + \cos(2\pi \times t \text{ days}/365 \text{ days})]$, and $T_{eq}^{winter}(\phi, \sigma)$ and $T_{eq}^{summer}(\phi, \sigma)$ are the midwinter and midsummer T_{eq}. A final warming can be identified in one seasonal cycle from winter to summer. SRC11 provide a detailed discussion on the simulations of final warmings.

Sudden warmings are simulated in a perpetual winter run, in which T_{eq} is fixed at its midwinter value. We use different T_{eq} for the simulations of sudden and final warmings: the radiative polar night jet parameter u_1 in Scott and Haynes (1998) is set to 280 m s^{-1} for the final warmings and as 200 m s^{-1} for the sudden warmings. The strength of the polar vortex is weaker in the perpetual winter run, allowing more and deeper sudden warmings to occur in the simulation, consistent with the sensitivities discussed by Gerber and Polvani (2009).

An idealized surface topography is applied only in the NH to represent the hemispheric asymmetry in the planetary wave forcing:

$$h(\lambda, \phi) = 4h_0 \mu^2 (1 - \mu^2) \sin(m\lambda), \quad (2)$$

where $\mu = \sin(\varphi)$, m is the zonal wavenumber, and h_0 is the topographic amplitude. SRC11 explored the downward influence of stratospheric final warming with different topographic amplitudes, zonal wavenumbers, polar vortex strengths, and horizontal resolutions and found that the downward influence of stratospheric seasonal transition is robust with respect to the model parameters. A detailed description of the model equations and other physical parameterizations can be found in Song and Robinson (2004) and SRC11.

The experiments described here are conducted with wavenumber-1 topography ($m = 1$). Taguchi et al. (2001) used this topography to force their model and found that the NH winter stratosphere corresponds to a high-amplitude topography regime, while the SH stratosphere is close to a low-amplitude regime. Similar results are found for the stratospheric seasonal transition in our model (Chen and Sun 2011). Here we use 1000- and 2000-m topography for the seasonal transition experiments, and 2000-m topography for the perpetual winter experiments. These experiments correspond to NH- and SH-like

TABLE 1. Mean and standard deviation of the onset dates for the 80-member final warmings with 1000- and 2000-m topographic amplitudes, and the onset dates of the selected 12 final warming cases used for the perturbation experiments. The onset dates are the number of days after the transition in the equilibrium temperature begins [t in Eq. (1) in the simulation].

h_0 (m)	Mean (days)	Std dev (days)	Selected final warming onset dates
1000	+134	11	Early: +97, +110, +111, +113
			Middle: +134, +134, +135, +135
			Late: +150, +150, +153, +158
2000	+101	19	Early: +58, +70, +70, +74
			Middle: +98, +99, +99, +102
			Late: +133, +141, +149, +157

stratospheric final warmings and stratospheric sudden warmings that occur frequently only in the NH.

b. Control warming events

Following BMR06 and Black and McDaniel (2007b), we define the final-warming onset with a threshold value of 50-hPa zonal wind at the latitude of the polar night jet. The onset of the final warming in the 2000-m topography experiments is the first day of the last time that the zonal mean zonal wind at 50 hPa at 70°N drops below zero without returning to 10 m s^{-1} until the fall, as for the observed NH final warmings. The definition of the final warming for the 1000-m case is similar but instead uses the zonal wind at 60°N and a 10 m s^{-1} threshold, as for the observed SH final warmings. Final warming events are obtained by first running 80 realizations of the seasonal cycle from winter to summer with the 1000- or 2000-m topography. The 80-member ensemble of final warmings is then divided into early, middle, and late final warmings according to the time of warming onset. In each of the three groups, four warming events are selected to compose 12 final warmings as the control runs for the predictability study. Table 1 gives the mean and standard deviation of the onset dates for the 80-member final warmings with 1000- and 2000-m topography and the onset dates for the 12 selected final warming cases used for the perturbation experiments.

In the perpetual-winter run with the 2000-m topography, the sudden warming onset is defined as the time when the zonal mean zonal wind at 10 hPa and 70°N becomes easterly. Here 70°N is adopted instead of 60°N in the World Meteorological Organization (WMO) definition, in order for the zonal wind to more easily transit to negative so that major sudden warmings occur in the model. If the interval between two sudden warmings is less than 30 days, they are categorized as one event. Because of the relatively weak vortex in the model, sudden warmings occur approximately once every 100 days. The

TABLE 2. Control and perturbation experiments for stratospheric final and sudden warmings.

Experiment	Description
Control run warming events	12 warming events selected for final warming or sudden warming.
Perturbation experiments	For each warming event, forecast experiments are initialized from day −10 and day −20 from the warming onset, with total, stratospheric, and tropospheric perturbations separately.
Zonally symmetric model	For the warming composite, forecast experiments are initialized from day −10 and day −20 from the warming onset, with perturbations in initial zonal flow and instantaneous eddy forcing separately.

first 1000 days of the perpetual winter run are discarded, and 12 sudden warmings are selected from the remaining 3000 days as the sudden warming control cases. The same definitions are used for each stratospheric warming event in the following perturbation experiments with the full model and the zonally symmetric model.

c. Perturbation experiments in the full model

For each stratospheric warming event, the predictability is evaluated by perturbing the initial conditions, and keeping all other settings unchanged from the control runs. Unlike an ensemble forecast with a number of random perturbations to initial conditions (e.g., Gerber et al. 2009), our perturbed initial conditions are taken from the same warming event but at a different time. For a forecast experiment starting at day t_i, the perturbed initial conditions are given by

$$X_{\text{perturb}}(t_i) = [1 - a(\sigma)]X_{\text{control}}(t_i) + a(\sigma)X_{\text{control}}(t_p). \quad (3)$$

Here $X_{\text{control}}(t)$ includes all the prognostic fields (i.e., the spectral fields of vorticity, divergence, temperature, and surface pressure in our spectral model) at the time t in the control simulation. The perturbed initial conditions $X_{\text{perturb}}(t_i)$ are determined by the perturbation time t_p and the function $a(\sigma)$ that determines what regions are perturbed. The perturbation experiments for the final warming and sudden warming events are summarized in Table 2 and described in detail as follows.

Forecast experiments are initialized from day $t_i = -20$ or −10 prior to the warming onset. The perturbation days t_p used for day −20 initial conditions are from day −29 to day −11, and the perturbation days for day −10 initial conditions are from day −19 to day −1, both with intervals of 2 days. Therefore, for each warming event, we have two control runs with day −20 and day −10 initial conditions, and for each initial condition, there are 10 perturbation experiments. Each perturbation run ends at day +40 with respect to the warming event in the control run. The design of the perturbation experiments is illustrated in Fig. 1.

We also performed forecast experiments with initial conditions much earlier than day −20 but found that the predictability of stratospheric warming events at these long leads is small. This is consistent with the results of Gerber et al. (2009), who showed that when the ensemble forecast starts from more than 20 days before the sudden warming onset, the forecasts exhibit considerable spread, and the warming is no longer predictable from initial conditions.

Three sets of forecast experiments are run, using total, stratospheric, and tropospheric perturbations according to different settings of $a(\sigma)$. In the total perturbation experiment, a is set to one everywhere, so that the perturbation field $X_{\text{control}}(t_p)$ completely replaces the original field $X_{\text{control}}(t_i)$. For sudden warmings, this forecast experiment is just a shift in time of X_{control} by $\delta t_i = t_p - t_i$, but for final warmings, the forecast experiment is also affected by the seasonally evolving radiative heating. This effect is small, however (section 3b). In the stratospheric perturbation experiments, a equals 1 for σ less than 0.1 and 0 for greater values, so only the stratosphere is perturbed. In the tropospheric experiment, on the other hand, $a(\sigma)$ equals 1 for σ larger than 0.1, and 0 in the stratosphere, so that only the troposphere is perturbed. The surface pressure perturbation is included with the tropospheric perturbations. The perturbations only in the stratosphere and troposphere will inevitably cause some dynamical adjustments after the initial conditions, these adjustments, however, are found to be small and do not affect the results.

One can understand the perturbed initial conditions by approximating Eq. (3) as

$$X_{\text{perturb}}(t_i) \approx X_{\text{control}}(t_i) + a(\sigma)\frac{\partial X_{\text{control}}(t_i)}{\partial t}\delta t_i, \quad (4)$$

where the shift in time is $\delta t_i = t_p - t_i$. For given initial time t_i, the change of warming onset time is a function of δt_i. Specifically, the earlier the perturbation time t_p before the initial condition t_i, the later the warming is likely to occur in the perturbation run than the control run. If we denote a shift of initial stratospheric fields in time by
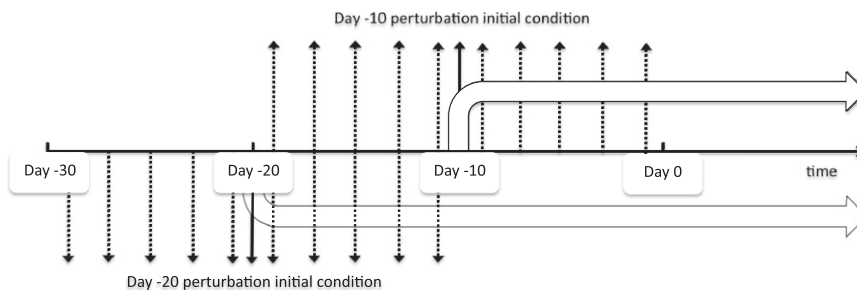
FIG. 1. The schematic illustration of the perturbation experiments for the stratospheric final warmings and sudden warmings. For each warming event, there are two control runs with the different initial conditions at day -20 and -10. The perturbation fields come from the same warming event but at a different time from the control run initial condition. All perturbation runs end at day $+40$.

δt_i^S and a shift of initial tropospheric fields in time by δt_i^T, the change of warming onset δt_0 can be approximated as

$$\delta t_0 \approx \frac{\partial t_0}{\partial t_i^S}\delta t_i^S + \frac{\partial t_0}{\partial t_i^T}\delta t_i^T. \qquad (5)$$

The effects of the stratosphere and troposphere on the predictability of the warming onset (i.e., $\partial t_0/\partial t_i^S$ and $\partial t_0/\partial t_i^T$) can be separately quantified by stratospheric or tropospheric perturbations. If the effects of the two contribute additively to the total perturbation, then $\partial t_0/\partial t_i^T + \partial t_0/\partial t_i^S = 1$.

d. Perturbation experiments in the zonally symmetric model

We use a zonally symmetric model to evaluate the different roles of the initial zonal mean flow and time-varying eddy forcing in determining the timing of stratospheric warming events. The zonally symmetric model uses the same radiative forcing and dissipation as the full model, but only the zonal mean circulation is retained, and the surface topography is included only through the eddy forcing. In this model, the eddy forcings are diagnosed from the daily output of the full model. A detailed description of this model can be found in the appendix of SRC11. The forecast experiments are done only for the composite of warming events. With the composite initial zonal mean flow and time-varying eddy forcings, we can approximately reproduce the composite zonal mean zonal wind evolutions in the full model.

For simplicity, the model can be thought of as $\partial \overline{X}(t)/\partial t = N[\overline{X}(t)] + E(t)$, where $\overline{X}(t)$ are the zonal mean prognostic variables, N is a nonlinear operator that describes the zonal symmetric model, and $E(t)$ is the eddy forcing at time t diagnosed from the full model. Analogous to the stratospheric and tropospheric perturbations in the full model experiments in Eq. (3), we separately perturb the timing of the initial zonal flow $\overline{X}(t_i)$ and

instantaneous eddy forcing $E(t)$ in the zonally symmetric model. In particular, initial zonal mean conditions are perturbed as the total perturbations in the full model, and the eddy forcings are shifted forward or backward in time for the entire time series. These two sets of experiments can be used to evaluate different roles of the initial mean flow and wave drag in determining the timing of stratospheric warmings. As we will show in section 3, they correspond to the roles of initial stratospheric and tropospheric perturbations in the full model.

3. Final warming results

a. Control warming events

The stratosphere final warming is the final collapse of the polar vortex in the spring as the solar heating increases in high latitudes. It appears as a polar warming and the reversal of zonal winds from wintertime westerlies to summertime easterlies (Andrews et al. 1987). In our simulations, as the final warming approaches, the winter polar vortex was displaced from the pole and then replaced by a summer high (not shown). This wave-1 transition pattern is similar to NH observations (Black and McDaniel 2007a). Figure 2 shows the evolutions of the 50-hPa high-latitude zonal wind and the E–P flux divergence for 12 final warmings and their composite (shown with asterisks) using 1000- and 2000-m topography. Both warmings are characterized by a large zonal wind deceleration around the onset time in the high-latitude stratosphere. Much of the deceleration can be attributed to a burst of planetary wave activity, which can be seen from the E–P convergence at 50 hPa and the E–P flux at 100 hPa (not shown). The final warming with 1000-m topography differs from the 2000-m final warming in that it has a much later onset date and the zonal wind transition is slower because of weaker planetary
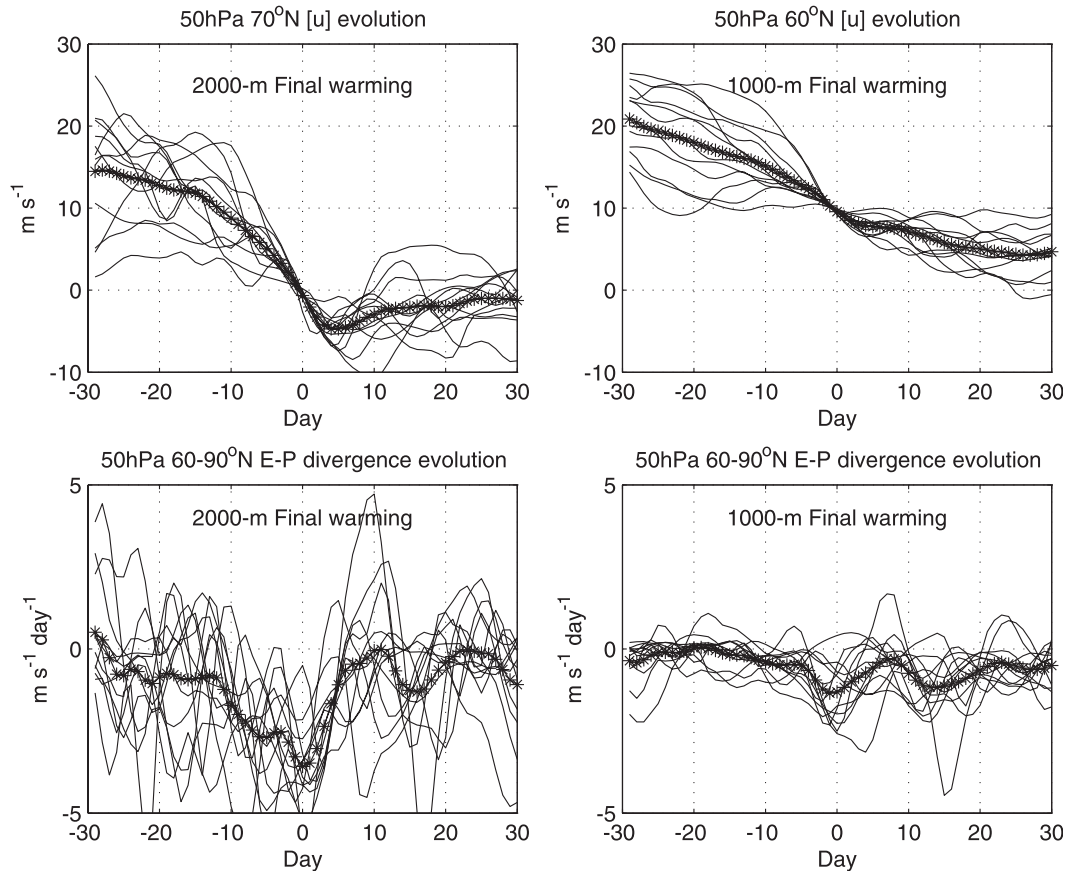
FIG. 2. (top) 50-hPa high-latitude composite zonal mean zonal wind evolutions for the final warmings with (left) 1000- and (right) 2000-m topographic forcings. (bottom) As at top, but for the 50-hPa composite E–P divergence. The asterisk line denotes the composite and the solid lines show all of the samples. The units for zonal wind and E–P divergence are m s^{-1} and m s^{-1} day^{-1}, respectively. The horizontal axis is the day with respect to the final warming onset date.

wave driving. These simulated final warmings are consistent with the observed differences between final warming events in the Northern and Southern Hemispheres (BMR06; Black and McDaniel 2007b).

b. Perturbation experiments

Total perturbation experiments are carried out by moving the initial conditions forward and backward in time, as in Eq. (3). The perturbation experiments are performed for each warming event, and then averaged over all the warmings and compared with the composite of the control warming. Figure 3 shows the evolution of the 50-hPa zonal-wind composite in the control (asterisks) and perturbation runs for final warmings with 2000-m topography. The left column of Fig. 3 shows the zonal wind changes with total perturbations in both the stratosphere and the troposphere. Following the change of the initial conditions, the zonal wind in the perturbed runs shifts forward and backward in time. The difference between

the experiments with day −20 and day −10 initial conditions can be attributed to the difference in the deceleration rate around the initial dates. Therefore, the timing of the final warming is completely determined by the shift of initial conditions in time and is unaffected by the timing of the event relative to the seasonal cycle. This is expected since the final warming is transient and occurs on a time scale much shorter than the seasonal cycle. This is also consistent with our understanding of the final warming as an essentially dynamical event, although it is initiated by the seasonal increase in solar heating.

The total perturbation experiments are compared with the experiments with stratospheric and tropospheric perturbations in the middle and right columns of Fig. 3. In the stratospheric perturbation experiments, the initial perturbed zonal wind departs from that in the control run, as is the case for the total perturbation experiments. In the experiments with day −20 initial conditions, the evolution of the zonal wind follows a deceleration rate
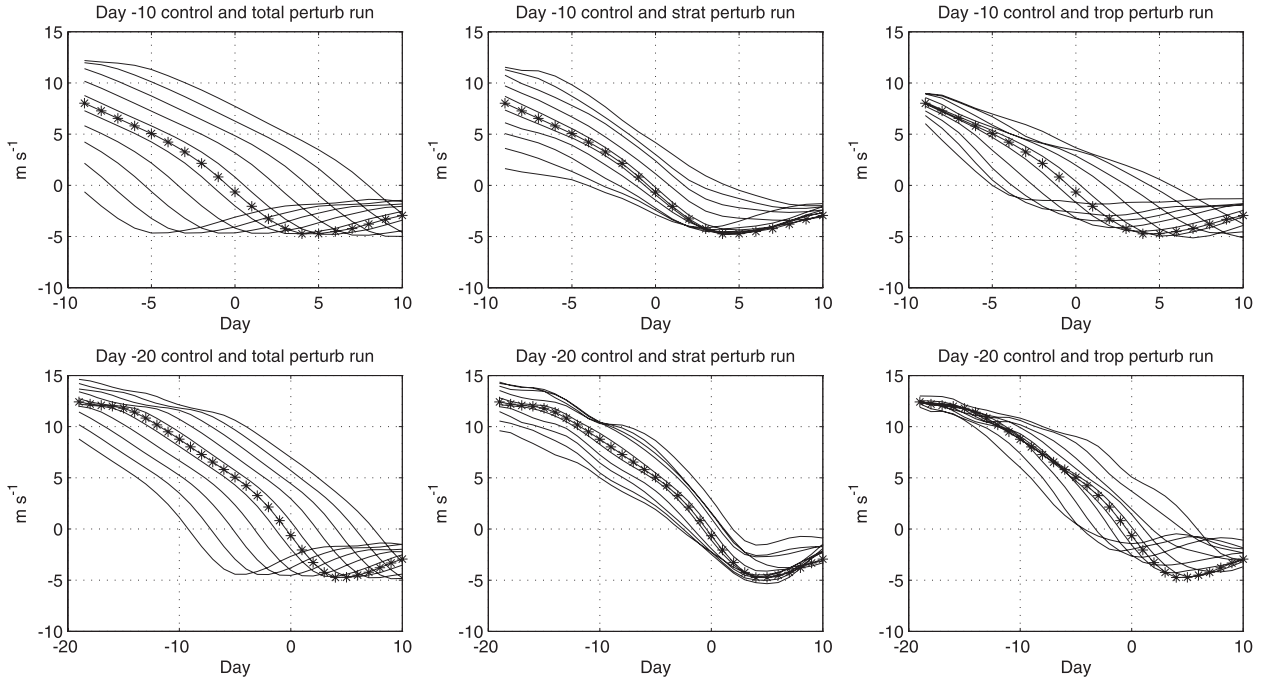
FIG. 3. 50-hPa 70°N zonal mean zonal wind evolutions of the composite control run (asterisk line) and 12-member ensemble-mean (left) total, (middle) stratospheric, and (right) tropospheric perturbation runs (solid line) for the final warmings with 2000-m topography, for the (top) day −10 control run and (bottom) day −20 control run. The perturbations used for day −20 initial conditions are the daily output from day −29 to day −11 while the perturbation fields for day −10 initial conditions are from day −19 to day −1, both with intervals of 2 days. The horizontal axis is the day with respect to the control run final warming onset date.

similar to the control run. The onset date ranges from day −5 to day +5 with respect to the onset date in the control run, compared to the range, from day −9 to day +9, in the total perturbation experiments. Similar differences are seen for the experiments with day −10 initial conditions. Therefore, the internal variability of the stratosphere does not explain all the predictability of the warming events. In contrast, in the tropospheric perturbation experiments, although all of the runs start from the same stratospheric initial condition, the stratospheric zonal wind deviates noticeably from the control run even 1 day after the initial conditions. The zonal wind reverses its sign earlier or later than in the control run, depending on the timing of the tropospheric initial conditions. This implies that the troposphere has a strong impact on the timing of the final warming. Roughly speaking, the zonal wind changes with stratospheric perturbations are nearly parallel to the control run, while the wind changes with tropospheric perturbations diverge from the control run. This suggests that both the stratosphere and troposphere influence the predictability of final warmings.

How does the change in initial stratospheric and tropospheric conditions affect the timing of the warming onset? Consider the zonal mean zonal wind change from t_i to the onset time t_0:

$$\overline{u}(t_0) - \overline{u}(t_i) = \int_{t_i}^{t_0} \frac{\partial \overline{u}(t)}{\partial t}\, dt = \left\langle \frac{\partial \overline{u}}{\partial t} \right\rangle (t_0 - t_i), \quad (6)$$

where $\overline{u}(t_0)$ is the threshold value of the zonal wind used to determine the warming onset (e.g., 0 or 10 m s^{-1}) and $\langle \partial \overline{u}/\partial t \rangle$ denotes the time mean deceleration rate from t_i to t_0. Equation (6) means that the zonal wind transition prior to the warmings can be expressed by the mean deceleration rate multiplied by the time it takes. From it, the change of the onset time t_0 can be expressed approximately as

$$\delta t_0 \approx -\frac{\delta \overline{u}(t_i)}{\langle \partial \overline{u}/\partial t \rangle} + \frac{\overline{u}(t_i) - \overline{u}(t_0)}{\langle \partial \overline{u}/\partial t \rangle^2} \delta \left(\left\langle \frac{\partial \overline{u}}{\partial t} \right\rangle \right). \quad (7)$$

Equation (7) says that changes in the timing of the final warming depend on changes in the initial stratospheric zonal flow $\overline{u}(t_i)$ and in the mean deceleration rate prior to the final warming $\langle \partial \overline{u}/\partial t \rangle$. Together with the quasi-geostrophic transformed Eulerian mean (TEM) momentum equation (e.g., Edmon et al. 1980),

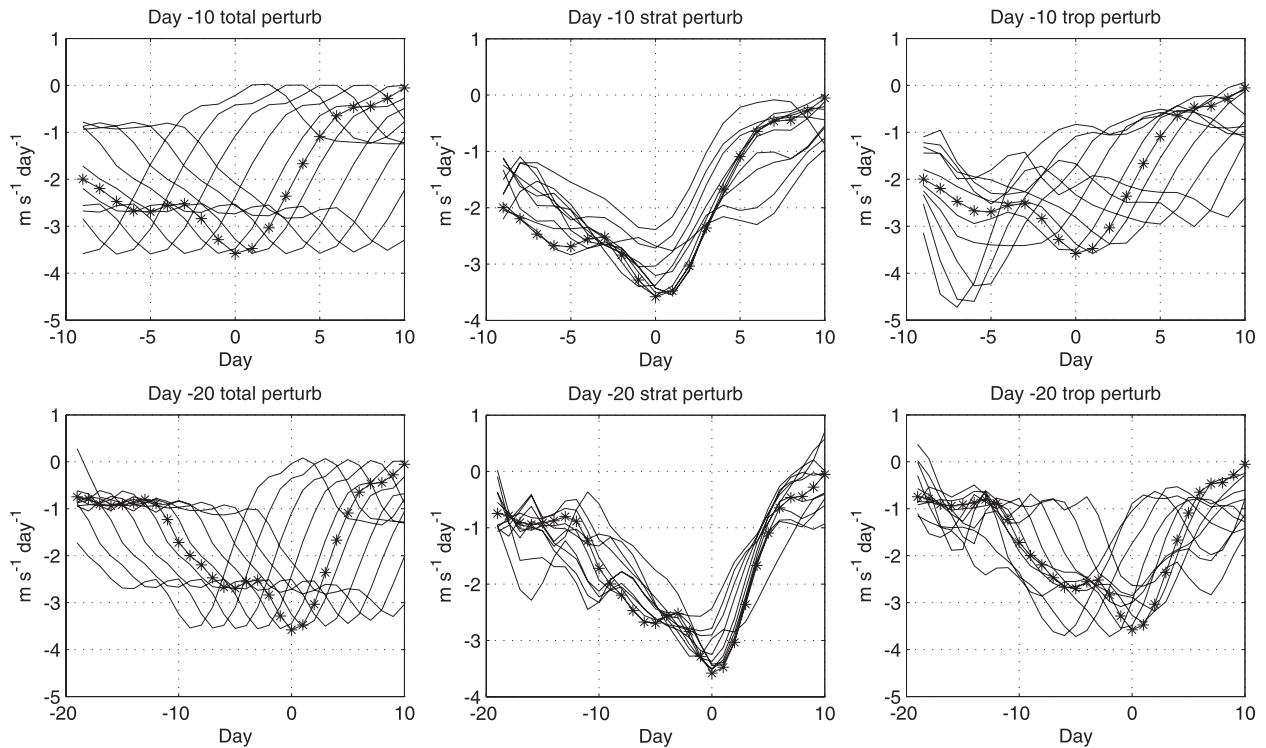$$\frac{\partial \overline{u}}{\partial t} - f \overline{v}^* = \nabla \cdot \mathbf{F}, \quad (8)$$

FIG. 4. 50-hPa 60°–90°N E–P divergence evolutions of the composite control run (asterisk line) and 12-member ensemble-mean (left) total, (middle) stratospheric, and (right) tropospheric perturbation runs (solid line) for the final warmings with 2000-m topography, for the (top) day −10 control run and (bottom) day −20 control run. The horizontal axis is the day with respect to the control run final warming onset date.

where f is the Coriolis parameter, $\bar{v}*$ is the residual meridional velocity, and $\mathbf{V} \cdot \mathbf{F}$ is the E–P divergence. This suggests that the timing of the final warming can be influenced by the stratosphere and the troposphere in two ways. The stratosphere provides the initial state of the zonal winds and thus partly determines the timing of the final warming. On the other hand, if the stratosphere and troposphere affect the wave drag prior to the final warming, this will also influence its timing. While the troposphere provides a source of stratospheric planetary waves, the stratosphere can modulate the flux of wave activity into the stratosphere. It is expected that both affect the evolution of wave drag in the stratosphere and thus influence the deceleration rate and the timing of the final warming.

We compare the evolution of the 50-hPa wave drag for the total, stratospheric, and tropospheric perturbations in Fig. 4. In the total perturbation experiments (Fig. 4, left) the wave drag and especially the timing of the maximum shift forward and backward in time, following the timing of the initial condition. This is similar to the changes of the wave drag in the tropospheric perturbation experiment in the right column, although the small differences in magnitude in these experiments are attributable to

influences from the stratospheric flow. In contrast, the wave drag in the stratospheric perturbation experiments in the middle column has a peak at the warming onset, similar to the control run, rather than shifting with the timing of stratospheric initial conditions. This indicates that the troposphere has a large impact on the rapid increase in wave drag in the stratosphere prior to the warming onset, while the modification of waves by the stratosphere is limited.

The zonal wind and wave drag results for 1000-m topography with stratospheric and tropospheric perturbations resemble those in the 2000-m experiments. Both stratospheric and tropospheric initial conditions are important for the predictability of final warming, and the evolution of stratospheric wave drag largely depends on tropospheric initial conditions. This suggests that the stratosphere affects the final warming onset in our model primarily not through the eddy–mean flow interactions in the stratosphere, but by the initial zonal wind.

c. Comparison with zonally symmetric model results

The preceding results show that the stratosphere and troposphere are important in determining the predictability of final warming events. Which one is more
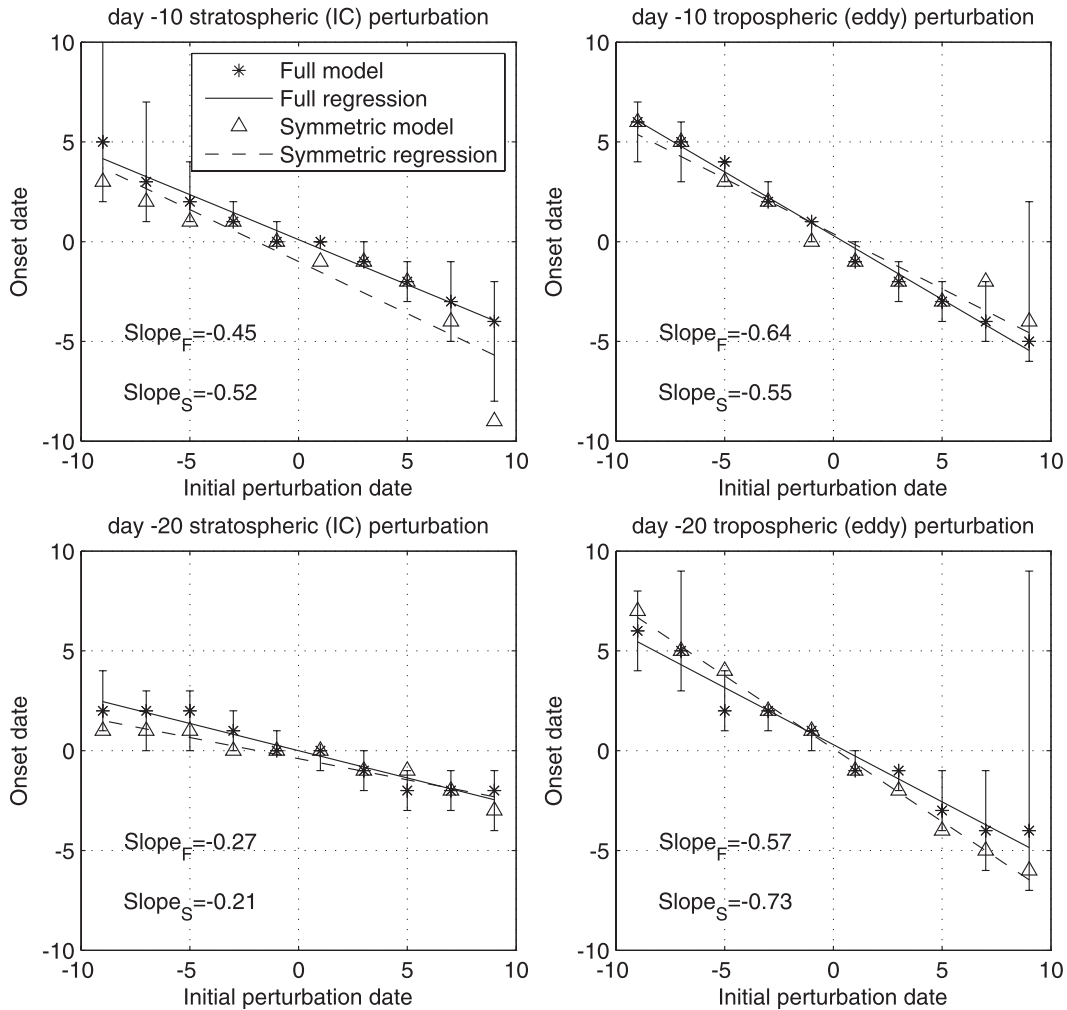
FIG. 5. Comparison of the stratospheric (tropospheric) perturbation experiments in the full model and the initial condition (eddy forcing evolution) perturbation experiments in the zonally symmetric model for the 2000-m final warming events, for the (top) day −10 control run and (bottom) day −20 control run. The horizontal axis indicates the day of the initial conditions [δt_i in Eq. (4)] or the shift in the time series of the eddy forcing, and the vertical axis shows the resulting onset dates, both with respect to the control run. The stratospheric and tropospheric perturbation results are denoted by asterisks and their linear regressions by solid lines. The error bar shows the onset dates for the Student's t test 95% confidence level of the zonal wind evolution deviated from the ensemble mean in the full model perturbation experiments. The initial condition and eddy forcing perturbation results are denoted by triangles and their linear regressions by dashed lines.

important? One way to quantify this is to consider the changes in the final warming onset date with the stratospheric or tropospheric perturbations [i.e., $\partial t_0/\partial t_i^S$ and $\partial t_0/\partial t_i^T$ in Eq. (5)]. For example, in the total perturbation experiments (Fig. 3, left), if the total perturbation initial condition is shifted backward (forward) in time by δt_i, the final warming onset date will be later (earlier) than in the control run by δt_i. This means that all the predictability is determined by the perturbation initial conditions. In a similar way, in the stratospheric and tropospheric experiments, shifting the initial condition can also change the final warming onset date, but

by a smaller amount, so that only part of the predictability is determined by the stratosphere or the troposphere separately.

Using the zonally symmetric model, we performed experiments similar to those described above, but now perturbing either the initial condition in the zonal flow or by shifting the evolution of the eddy forcing in time. Since the eddy forcing is imposed in the zonally symmetric model, perturbing the initial condition does not affect its evolution. Therefore, in the zonally symmetric model, the timing of the warming can be determined by the initial condition, which provides a starting point for
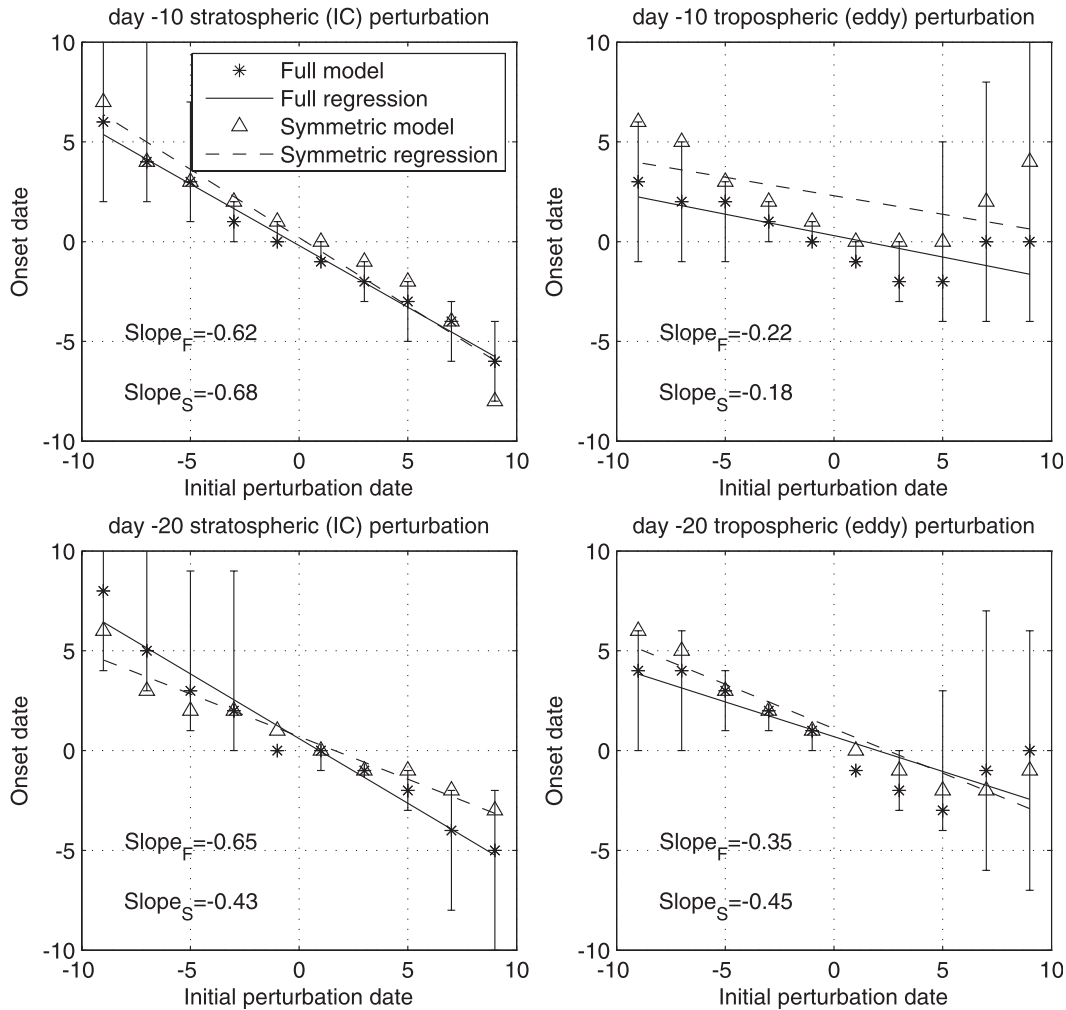
FIG. 6. As in Fig. 5, but for the 1000-m topographic final warming events.

the deceleration of the zonal flow, and by the evolution of eddy forcing, which determines the zonal wind deceleration prior to the final warming. We can compare the initial perturbation results in the zonally symmetric model with the stratospheric perturbation results in the full model. Since the modification of the waves by the initial stratospheric zonal flow is limited (Fig. 4, middle), we expect that the changes in the onset dates should be similar. Also, since troposphere largely determines the evolution of the eddy forcing in the stratosphere, we expect that shifting the eddy forcing in the zonally symmetric model will give similar results to the tropospheric perturbations in the full model.

Figure 5 shows warming onset dates for the 2000-m final warmings with initial conditions perturbed separately in the stratosphere and troposphere in the full model, with the results for perturbing the initial conditions and eddy forcings in the zonally symmetric model. The error bar indicates the onset dates for the two-sided

Student's t test 95% confidence levels of the zonal wind evolution deviated from the ensemble mean in the perturbation experiments.

For some perturbation experiments, zonal winds do not drop below the threshold value. At this time, we use the day of minimum zonal wind to represent the warming onset date. The abscissa indicates the day of the initial conditions [δt_i in Eq. (4)] or the shift in the time series of the eddy forcing, and the ordinate shows the resulting onset dates, both with respect to the control run. For the day −20 and day −10 initial conditions, when the tropospheric or stratospheric initial conditions are shifted backward some number of days from the control run, the final warming onset dates are later than in the control run, and vice versa. The changes in onset date, however, are smaller than the shifts in the initial conditions. This implies that both the stratosphere and the troposphere control the timing of the final warming. The slopes for the tropospheric perturbations are larger. The sum of

the two slopes deviates from 1, which can be attributed to the nonlinear terms ignored in Eq. (4) in separating the troposphere and stratosphere. Also, the slope for the day -10 stratospheric perturbation is -0.45, greater than -0.27, the slope for the day -20 experiments. The stratosphere is responsible for more of the predictability of the final warming as the onset date approaches. The slopes for the tropospheric perturbations at day -10 and day -20 are, however, similar.

There is a close correspondence, in Fig. 5, between perturbing the zonal initial conditions in the zonally symmetric model and perturbing the stratospheric initial conditions in the full model, and likewise between shifting the eddy forcing in the zonally symmetric model and perturbing the tropospheric initial conditions in the full model. This indicates that the modification of the wave drag by the stratospheric zonal flow has only a limited effect on the timing of the final warming. This confirms our finding that the troposphere has a large impact on the stratospheric wave drag, which thus affects the zonal wind deceleration and the date of the final warming, while the stratosphere influences the timing of the final warming primarily by providing the initial state of the zonal winds.

Figure 6 shows the results in the full model and the zonally symmetric model for the final warmings with 1000-m topography. As in Fig. 5, the results for stratospheric and tropospheric perturbations to the initial conditions in the full model are similar to the results for perturbing the zonal initial conditions and shifting eddy forcing in the zonally symmetric model. In comparison with the results for 2000-m topography, the stratosphere has a greater influence on the timing of the final warming than the troposphere. This is a consequence of the more gradual deceleration of the zonal winds in cases with weaker topography (Fig. 2). For example, at day -20, the zonal wind change by temporal shift between weak and strong topographic cases are similar. Then the small deceleration rate in the weak topographic cases corresponds to a larger temporal deviation from the control run, leading to a larger role for the stratospheric initial condition in determining the timing of warming.

4. Sudden warming results

a. Control warming events

Stratospheric sudden warmings in our simulation resemble the "vortex displacement" events in NH observations (Charlton and Polvani 2007), in which wave 1 amplifies as the warming approaches. Figure 7 shows the high-latitude zonal mean zonal wind and E–P divergence for 12 sudden warmings and their composite from the perpetual winter control run. These are similar to the
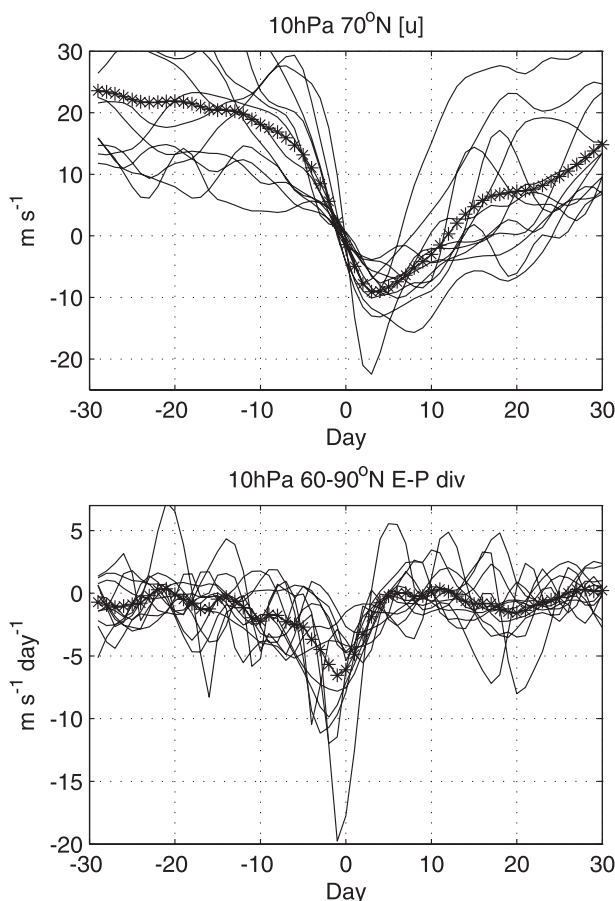

FIG. 7. (top) 10-hPa 70°N composite zonal mean zonal wind evolutions for the sudden warming events. (bottom) As at top, but for the 10-hPa 60°–90°N E–P divergence. The asterisk line denotes the composite and the solid lines show all the samples. The units for zonal wind and E–P divergence are m s^{-1} and m s^{-1} day^{-1}, respectively. The horizontal axis is the day with respect to the final warming onset date.

results for final warmings shown in Fig. 2, but here we display results at 10 hPa, the level used to define the sudden warming. The zonal wind transition in the sudden warming is similar to the final warming, but with a more rapid deceleration of the zonal winds, due to the stronger wave amplification around the onset date. In our sudden warmings, an investigation of the planetary wave refractive index (not shown) does not suggest the existence of a subtropical propagation barrier, which has been proposed as a mechanism by which stratospheric "preconditioning" leads to a focusing of wave activity into the vortex (McIntyre 1982). This could be because we have used only wave-1 topographic forcing, and thus only wave-1 warmings. Stratospheric preconditioning may be more relevant to "vortex-splitting" sudden warmings than to vortex displacement warmings, as had been found in observations (Charlton and Polvani
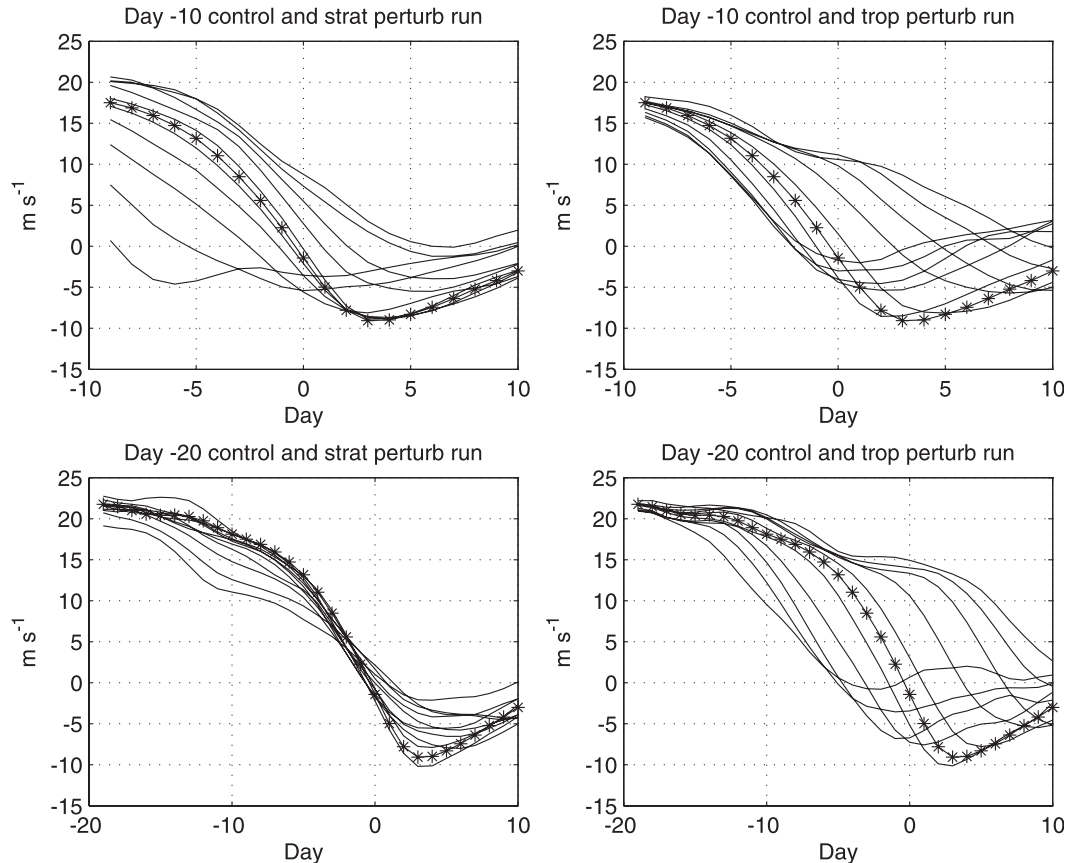
FIG. 8. 10-hPa 70°N zonal mean zonal wind evolutions of the composite control run (asterisk line) and 12-member ensemble-mean perturbation runs (solid line) for the sudden warming events, for the (left) stratospheric and (right) tropospheric perturbation experiments, for the (top) day −10 control run and (bottom) day −20 control run. The horizontal axis is the day with respect to the control run final warming onset date.

2007) and in simulations (Mukougawa and Hirooka 2004).

b. Perturbation experiments

Perturbation experiments are performed for 12 sudden warming events, as for the final warmings. Because the radiative equilibrium temperature is constant with time in the perpetual winter run, the total perturbation is merely to shift the sudden warming backward or forward in time, so only tropospheric and stratospheric perturbation experiments are performed. Figure 8 shows the composite zonal wind changes for perturbing stratospheric and tropospheric initial conditions. As for the final warmings, the stratospheric perturbation experiments show different initial winds but a similar deceleration rate, while the tropospheric perturbation experiments show a diverging pattern from the same initial winds. For day −10 initial conditions, both the stratosphere and troposphere contribute to the timing of the warming, but for day −20 initial conditions, the troposphere is more important.

c. Comparison with zonally symmetric model results

Figure 9 shows the onset dates for the stratospheric and tropospheric perturbations, together with the results from the zonally symmetric model, perturbing the initial conditions and temporally shifting the eddy forcing. The results for perturbing the tropospheric initial conditions in the full model again resemble those for shifting the eddy forcing in the zonally symmetric model, consistent with the expectation that tropospherically forced planetary waves drive the dynamics of sudden warmings. For day −20 initial conditions, the stratosphere has very little influence on the timing of sudden warmings in the full model and in the zonally symmetric model. Figure 9 shows that at day −20 the stratospheric zonal winds have barely begun their deceleration, so shifting the timing of the initial conditions around day −20 has little effect on the initial stratospheric zonal winds.

Closer to the warming, for day −10 initial conditions, the slope for perturbing the stratospheric initial conditions is much greater than that resulting from changes in
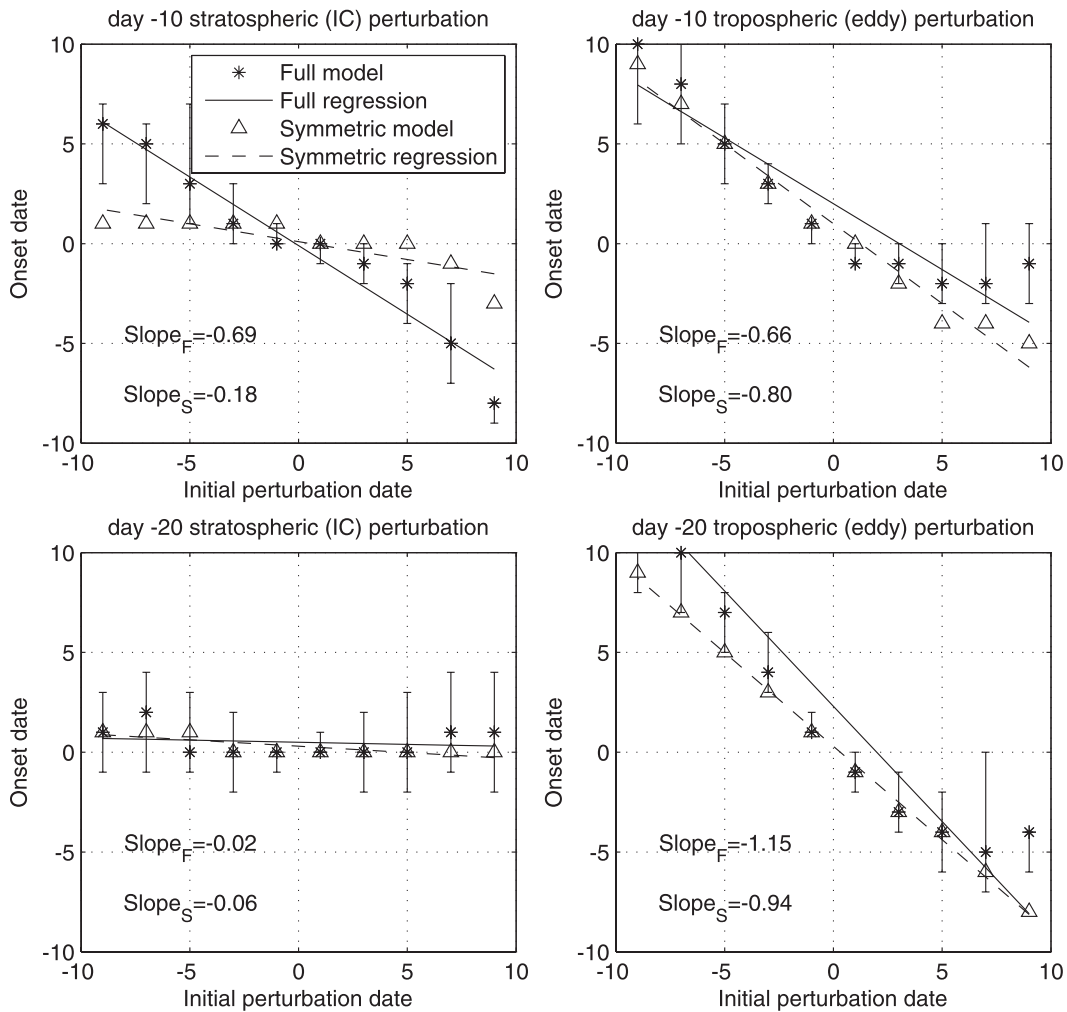
FIG. 9. As in Fig. 5, but for the sudden warming events. The horizontal axis indicates the day of the initial conditions [δt_i in Eq. (4)] or shift in the time series of the eddy forcing, and the vertical axis shows the resulting onset dates, both with respect to the control run, for the (top) day -10 control run and (bottom) day -20 control run. The stratospheric and tropospheric perturbation results are denoted by asterisks and their linear regressions by solid lines. The error bar shows the onset dates for the Student's t test 95% confidence level of the zonal wind evolution deviated from the ensemble mean in the full model perturbation experiments. The initial condition and eddy forcing perturbation results are denoted by triangles and their linear regressions are denoted by dashed lines.

the zonal initial condition in the zonally symmetric model. This differs from the results for other times in the sudden warmings and for the final warmings and suggests that, close to the warming onset, the stratospheric zonal flow significantly influences the wave drag in the stratosphere.

The stratospheric eddy feedback for the day -10 sudden warming experiments is illustrated in Fig. 10 using the experiment with the perturbation day $t_p = -5$. The top panel shows the zonal winds at 10 hPa, 70°N for the control run, the stratospheric perturbation experiment in the full model, and the initial condition perturbation with no change in eddy forcing in the zonally symmetric

model. Since the zonally symmetric model is forced by the same eddy forcing as in the control warming events, the zonal winds in the zonally symmetric model follow the zonal wind changes in the control run, with a slightly different deceleration, due to the adjustment by the residual circulation. For stratospheric perturbations in the full model, however, the zonal wind deceleration is initially larger than the deceleration in the zonally symmetric model, and therefore the final warming occurs earlier.

This increased deceleration rate results from greater E–P convergence, which is shown in the bottom panel. As the zonal wind decreases due to the initial stratospheric
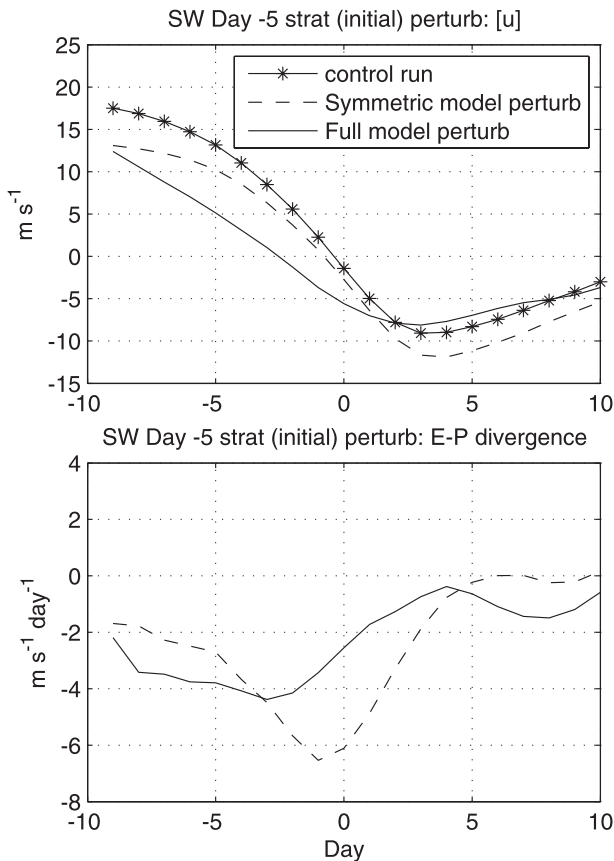
FIG. 10. (top) 10-hPa 70°N zonal mean zonal wind for the day −5 initial condition perturbation experiment in the zonally symmetric model and day −5 stratospheric perturbation experiment in the full model. (bottom) As at top, but for the 10-hPa 60°–90°N averaged E–P divergence. The unit of zonal wind is m s^{-1}. The unit of E–P divergence is m s^{-1} day^{-1}.

perturbation, the convergence of the E–P flux increases in the first week of the perturbation experiments. This provides a positive feedback on the deceleration of the stratospheric zonal winds and leads to a more rapid onset of the warming. After the final warming, however, stationary planetary waves can no longer propagate into the stratosphere, and the westward wave driving is reduced in comparison with the control. We performed similar analyses for different perturbation days from $t_p =$ day −1 to $t_p =$ day −19 and found similar positive feedbacks, indicating strong eddy–mean flow interaction close to the warming onset.

This feedback, however, is not evident in the day −20 initial conditions for the sudden warmings and all of the final warmings (not shown), even though the modification of the waves by the stratospheric zonal flow is clear (Fig. 4, middle). In other words, the modification of stratospheric wave driving is not sufficient to alter the zonal flow vacillation except when the initial condition is

very close to warmings at lead times greater than a few weeks.

For day −20 initial conditions, our results indicate that almost all of the potential predictability of sudden warmings in our model comes from the troposphere. To test this, we select one sudden warming day −20 control run, and use day −60 initial conditions from the 12 sudden warmings to perturb the stratosphere. The 12-member ensemble mean zonal wind gives an onset date close to the control run. We also perturb the troposphere in a similar way, and in this case the sudden warming does not occur in the ensemble mean. This supports our previous results that troposphere is crucial for the predictability of sudden warmings at lead times of greater than a few weeks.

5. Discussion and conclusions

The relative roles of stratospheric and tropospheric initial conditions in determining the timing of Southern and Northern Hemisphere-like stratospheric final warmings and stratospheric sudden warmings are evaluated using an idealized atmospheric model. Forecast experiments initialized from 10 and 20 days prior to warmings are separately perturbed in the troposphere and in the stratosphere. It is found that the stratosphere affects predictions of warming onset primarily by providing the initial state of the zonal winds, while the troposphere has a large impact through the generation and propagation of planetary waves. These results correspond to the roles played by the initial conditions and eddy forcings in a zonally symmetric model. The initial stratospheric zonal flow influences stratospheric wave driving, but generally this does not significantly affect the timing of the warming onset, except for initial conditions very close to the onset date.

In our perturbation experiments, the initial stratospheric flow is most important in determining the timing of warming in the 1000-m final warming, less so in the 2000-m final warming, and least important for the sudden warmings, whereas the importance of the tropospheric initial condition ranks in reverse order. This has some connection with the wave drag prior to the warming events. The stronger it is, the more rapid the deceleration of the stratospheric zonal wind. Therefore, given a similar magnitude of stratospheric perturbation, the change in the warming date will be smaller, reducing the stratospheric influence on the timing of the warming. This neglects, however, the role of stratospheric eddy feedback, as is seen for the stratospheric perturbations to day −10 initial conditions in our sudden warming cases. At this time, the stratosphere can modify the wave drag, so that the stratospheric role in determining the timing of the warming is increased. Other cases also

exhibit some stratospheric modification of the wave drag, but with a limited effect on the deceleration of stratospheric zonal winds and, thus, on the timing of the warmings. Overall, our results highlight the tropospheric role in producing stratospheric wave drag and providing predictability for sudden warmings. They support the importance of tropospheric precursors to the stratospheric events.

Our experiments suggest that stratospheric preconditioning plays a secondary role in the warming onset, at least for wavenumber-1 vortex breakdowns. The sudden warming can be classified into "vortex displacement" and "vortex-splitting" events. Observational analyses indicate that the two types of warmings are dynamically distinct (Charlton and Polvani 2007), despite the similar influence on the troposphere. The predictabilities of two types of warmings also differ. The predictability for the vortex-splitting event is normally 1 week or so (Allen et al. 2006), much shorter than several weeks for the vortex displacement event (Mukougawa and Hirooka 2004). Nevertheless, the important role of the troposphere is seen in both types of sudden warmings (Mukougawa and Hirooka 2004; Allen et al. 2006). Our results for wavenumber-1 sudden warmings are consistent with these studies.

REFERENCES

Allen, D. R., L. Coy, S. D. Eckermann, J. P. McCormack, G. L. Manney, T. F. Hogan, and Y.-J. Kim, 2006: NOGAPS-ALPHA simulations of the 2002 Southern Hemisphere stratospheric major warming. *Mon. Wea. Rev.,* **134,** 498–518.

Andrews, D. G., J. R. Holton, and C. B. Leovy, 1987: *Middle Atmosphere Dynamics.* Academic Press, 489 pp.

Baldwin, M. P., and T. J. Dunkerton, 2001: Stratospheric harbingers of anomalous weather regimes. *Science,* **294,** 581–584.

——, D. B. Stephenson, D. W. J. Thompson, T. J. Dunkerton, A. J. Charlton, and A. O'Neill, 2003: Stratospheric memory and skill of extended-range weather forecasts. *Science,* **301,** 636–640.

Black, R. X., and B. A. McDaniel, 2007a: The dynamics of Northern Hemisphere stratospheric final warming events. *J. Atmos. Sci.,* **64,** 2932–2946.

——, and ——, 2007b: Interannual variability in the Southern Hemisphere circulation organized by stratospheric final warming events. *J. Atmos. Sci.,* **64,** 2968–2975.

——, ——, and W. A. Robinson, 2006: Stratosphere–troposphere coupling during spring onset. *J. Climate,* **19,** 4891–4901.

Charlton, A. J., and L. M. Polvani, 2007: A new look at stratospheric sudden warmings. Part I: Climatology and modeling benchmarks. *J. Climate,* **20,** 449–469.

——, A. O'Neill, D. B. Stephenson, W. A. Lahoz, and M. P. Baldwin, 2003: Can knowledge of the state of the stratosphere be used to improve statistical forecasts of the troposphere? *Quart. J. Roy. Meteor. Soc.,* **129,** 3205–3224.

Chen, G., and L. Sun, 2011: Mechanisms of the tropical upwelling branch of the Brewer–Dobson circulation: The role of extratropical waves. *J. Atmos. Sci.,* **68,** 2878–2892.

Christiansen, B., 1999: Stratospheric vacillation in a general circulation model. *J. Atmos. Sci.,* **56,** 1858–1872.

——, 2000: Chaos, quasiperiodicity, and interannual variability: studies of a stratospheric vacillation model. *J. Atmos. Sci.,* **57,** 3161–3173.

Edmon, H. J., B. J. Hoskins, and M. E. McIntyre, 1980: Eliassen–Palm cross sections for the troposphere. *J. Atmos. Sci.,* **37,** 2600–2616.

Garfinkel, C. I., D. L. Hartmann, and F. Sassi, 2010: Tropospheric precursors of anomalous Northern Hemisphere stratospheric polar vortices. *J. Climate,* **23,** 3282–3299.

Gerber, E. P., and L. M. Polvani, 2009: Stratosphere–troposphere coupling in a relatively simple AGCM: The importance of stratospheric variability. *J. Climate,* **22,** 1920–1933.

——, C. Orbe, and L. M. Polvani, 2009: Stratospheric influence on the tropospheric circulation revealed by idealized ensemble forecasts. *Geophys. Res. Lett.,* **36,** L24801, doi:10.1029/2009GL040913.

Held, I. M., and M. J. Suarez, 1994: A proposal for the intercomparison of the dynamical cores of atmospheric general circulation models. *Bull. Amer. Meteor. Soc.,* **75,** 1825–1830.

Holton, J. R., and C. Mass, 1976: Stratospheric vacillation cycle. *J. Atmos. Sci.,* **33,** 2218–2225.

Kuroda, Y., 2008: Role of the stratosphere on the predictability of medium-range weather forecast: A case study of winter 2003–2004. *Geophys. Res. Lett.,* **35,** L19701, doi:10.1029/2008GL034902.

Kushner, P. J., and L. M. Polvani, 2004: Stratosphere–troposphere coupling in a relatively simple AGCM: The role of eddies. *J. Climate,* **17,** 629–639.

Labitzke, K., 1981: The amplification of height wave 1 in January 1979: A characteristic precondition for the major warming in February. *Mon. Wea. Rev.,* **109,** 983–989.

Marshall, A. G., and A. A. Scaife, 2010: Improved predictability of stratospheric sudden warming events in an atmospheric general circulation model with enhanced stratospheric resolution. *J. Geophys. Res.,* **115,** D16114, doi:10.1029/2009JD012643.

Martius, O., C. Schwierz, and H. C. Davies, 2009: Blocking precursors to stratospheric sudden warming events. *Geophys. Res. Lett.,* **36,** L14806, doi:10.1029/2009GL038776.

McIntyre, M. E., 1982: How well do we understand the dynamics of stratospheric warmings? *J. Meteor. Soc. Japan,* **60,** 37–65.

Mukougawa, H., and T. Hirooka, 2004: Predictability of stratospheric sudden warming: A case study for 1998/99 winter. *Mon. Wea. Rev.,* **132,** 1764–1776.

Polvani, L. M., and D. W. Waugh, 2003: Upward wave activity flux as a precursor to extreme stratospheric events and subsequent anomalous surface weather regime. *J. Climate,* **17,** 3548–3554.

Reichler, T., P. J. Kushner, and L. M. Polvani, 2005: The coupled stratosphere–troposphere response to impulsive forcing from the troposphere. *J. Atmos. Sci.,* **62,** 3337–3352.

Robinson, W. A., 1986: The behavior of planetary wave 2 in preconditioned zonal flows. *J. Atmos. Sci.,* **43,** 3109–3121.

Roff, G., D. W. J. Thompson, and H. Hendon, 2011: Does increasing model stratospheric resolution improve extended-range

forecast skill? *Geophys. Res. Lett.,* **38,** L05809, doi:10.1029/2010GL046515.

Salby, M. L., and P. F. Callaghan, 2007: Influence of planetary wave activity on the stratospheric final warming and spring ozone. *J. Geophys. Res.,* **112,** D20111, doi:10.1029/2006JD007536.

Scinocca, J. F., and P. H. Haynes, 1998: Dynamical forcing of stratospheric planetary waves by tropospheric baroclinic eddies. *J. Atmos. Sci.,* **55,** 2361–2392.

Scott, R. K., and P. H. Haynes, 1998: Internal interannual variability of the extratropical stratospheric circulation: The low-latitude flywheel. *Quart. J. Roy. Meteor. Soc.,* **124,** 2149–2173.

——, and L. M. Polvani, 2004: Stratospheric control of upward wave flux near the tropopause. *Geophys. Res. Lett.,* **31,** L02115, doi:10.1029/2003GL017965.

——, and ——, 2006: Internal variability of the winter stratosphere. Part I: Time-independent forcing. *J. Atmos. Sci.,* **63,** 2758–2776.

Song, Y., and W. A. Robinson, 2004: Dynamical mechanisms for stratospheric influences on the troposphere. *J. Atmos. Sci.,* **61,** 1711–1725.

Sun, L., and W. A. Robinson, 2009: Downward influence of stratospheric final warming events in an idealized model. *Geophys. Res. Lett.,* **36,** L03819, doi:10.1029/2008GL036624.

——, ——, and G. Chen, 2011: The role of planetary waves in the downward influence of stratospheric final warming events. *J. Atmos. Sci.,* **68,** 2826–2843.

Taguchi, M., T. Yamaga, and S. Yoden, 2001: Internal variability of the troposphere–stratosphere coupled system simulated in a simple global circulation model. *J. Atmos. Sci.,* **58,** 3184–3203.

Waugh, D. W., W. J. Randel, S. Pawson, P. A. Newman, and E. R. Nash, 1999: Persistence of the lower stratospheric polar vortices. *J. Geophys. Res.,* **104,** 27 191–27 201.

Yoden, S., 1987: Bifurcation properties of a stratospheric vacillation model. *J. Atmos. Sci.,* **44,** 1723–1733.